

# Solvothermal synthesis of $\chi\%$ TiO<sub>2</sub>/HZSM-5 and photocatalytic degradation of methyl orange

YUFENG SUN<sup>a</sup>, ZHENG MA<sup>a</sup>, XIJUAN CHEN<sup>a,b</sup>, WENJIE ZHANG<sup>a,\*</sup>

<sup>a</sup>*School of Environmental and Chemical Engineering, Shenyang Ligong University, Shenyang 110159, China*

<sup>b</sup>*State Key Laboratory of Forest and Soil Ecology, Institute of Applied Ecology, Chinese Academy of Sciences, Shenyang 110164, China*

Solvothermal method was used to synthesize composite  $\chi\%$ TiO<sub>2</sub>/HZSM-5 for degradation of methyl orange. Nano sized anatase TiO<sub>2</sub> was loaded on the surface of HZSM-5. The supported  $\chi\%$ TiO<sub>2</sub>/HZSM-5 has larger surface area than pure TiO<sub>2</sub>, depending on TiO<sub>2</sub> loading content. Smaller pore size and larger total pore volume are obtained after the addition of HZSM-5. Adsorption of methyl orange on the materials is around 5% while photocatalytic degradation is the major decoloration way. 40%TiO<sub>2</sub>/HZSM-5 has the maximum activity that is as high as 53% after 30 min of irradiation.

(Received November 23, 2015; accepted November 25, 2016)

**Keywords:** TiO<sub>2</sub>, Photocatalytic, HZSM-5, Solvothermal

## 1. Introduction

TiO<sub>2</sub>-based materials have been widely applied in photocatalytic decomposition of environmental pollutants [1-3]. An obstacle of using powder materials in large scale cleaning of wastewater is the reuse of photocatalyst after treatment. Since filtrating of very fine powders from the treated water is not feasible, various supported forms are adopted for the possible industrial application. Many kinds of materials such as glass [4], graphite [5], and SiO<sub>2</sub> [6] are investigated for this purpose. The satisfactory industrial application of zeolite as adsorbent and catalyst makes it a potential support for photocatalytic materials. Charge transfer process is observed in the Si-Al skeleton of porous zeolite caves [7]. Several typical types of zeolites, such as Y, ZSM-5, and MCM-41 [8-15], have been studied to support titanium dioxide with improved activity in wastewater treatment.

Solvothermal method has been used to prepare TiO<sub>2</sub>-based materials [16,17]. However, it is a new approach to synthesize supported TiO<sub>2</sub>. In this work, solvothermal method was used to synthesize the composite TiO<sub>2</sub>/HZSM-5. X-ray diffraction pattern, scanning electron microscope image, specific surface area, and porosity of the  $\chi\%$ TiO<sub>2</sub>/HZSM-5 composites were measured to describe the effect of TiO<sub>2</sub> loading content on physico-chemical properties of the materials. Methyl orange solution was chosen as a wastewater to study photocatalytic activity of the  $\chi\%$ TiO<sub>2</sub>/HZSM-5 composites.

## 2. Experimental

### 2.1. Material preparation

A solvothermal method was used to synthesize TiO<sub>2</sub> supported on HZSM-5. 0.6 mL ultrapure water and 3 mL anhydrous ethanol were mixed together. 2 mL tetrabutyl titanate, 0.04 mL acetylacetone, 0.1 mL hydrochloric acid, and HZSM-5 were mixed with 6 mL anhydrous ethanol under stirring to form a suspension. The former solution was subsequently dropped into the latter suspension, and the resulting suspension was transferred into a 50 mL PTFE container that situated in a high pressure stainless reactor. The solvothermal reaction was conducted at 180 °C for 24 hrs. After cooling to ambient temperature, the solid product was filtrated and dried at 80 °C for 7 hrs. The powders were heated in a furnace with a heating rate of 5 °C/min, and then maintained at 450 °C for 2 hrs. The produced materials were named as  $\chi\%$ TiO<sub>2</sub>/HZSM-5, where  $\chi\%$  was weight content of TiO<sub>2</sub> in the composites. The un-supported TiO<sub>2</sub> powders were prepared in the similar route without using HZSM-5.

### 2.2. Characterization of the material

X-ray diffraction patterns of the materials were measured using D/max-rB with a Cu K $\alpha$  source. Lattice parameters were calculated from XRD data using the analytical software Jade 5.0. Scanning electron microscope images were taken on a Hitachi S-3400N. An F-Sorb 3400 instrument was used to measure specific surface area and porosity of the materials.

### 2.3. Photocatalytic reaction

Photocatalytic activity of the materials was measured in a lab-made reactor using methyl orange solution as the wastewater. The UV light source can irradiate at 253.7 nm with the intensity of 1200  $\mu\text{W}/\text{cm}^2$ . 50 mL of 10 mg/L methyl orange solution and 30 mg  $\text{TiO}_2$  were stirred in the reactor to determine the adsorption of methyl orange on the photocatalysts in prior to turn on the light. Methyl orange concentration was measured by a UV-Vis spectrophotometer according to Lamb-Beer theory.

### 3. Results and discussion

Solvothermal method is usually used to prepare  $\text{TiO}_2$  as a photocatalyst. Fig. 1 shows XRD patterns of  $\chi\% \text{TiO}_2/\text{HZSM-5}$  with different  $\text{TiO}_2$  loading content. Both of the XRD patterns of anatase  $\text{TiO}_2$  and HZSM-5 can be distinguished in the figure, while diffraction intensities of anatase  $\text{TiO}_2$  grows with increasing  $\text{TiO}_2$  loading content. The diffraction peaks of the (101) plane of anatase  $\text{TiO}_2$  is used to calculate crystallite size of  $\text{TiO}_2$  based on Scherrer's formula. The crystallite sizes of  $\text{TiO}_2$  in the samples 30% $\text{TiO}_2/\text{HZSM-5}$ , 40% $\text{TiO}_2/\text{HZSM-5}$ , and 60% $\text{TiO}_2/\text{HZSM-5}$  are 8.05 nm, 7.89 nm, and 7.81 nm, respectively. The loaded  $\text{TiO}_2$  is in the nano size on the surface of HZSM-5.

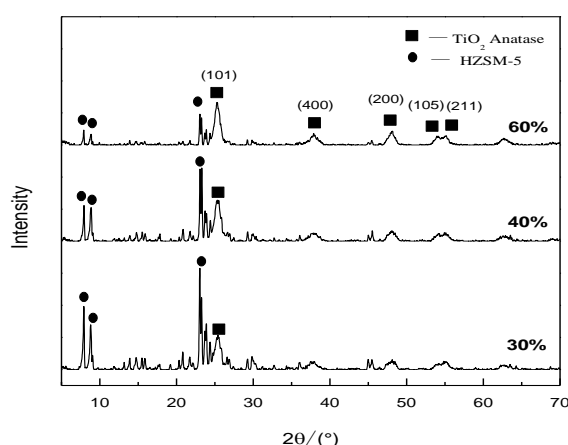


Fig. 1. XRD patterns of  $\chi\% \text{TiO}_2/\text{HZSM-5}$  with different loading content

SEM images of the supported  $\chi\% \text{TiO}_2/\text{HZSM-5}$  are shown in Fig. 2. The regular shape of HZSM-5 can still be found in Fig. 2(a) of 30% $\text{TiO}_2/\text{HZSM-5}$  that contains only 30% of  $\text{TiO}_2$ . Most of the surface of HZSM-5 particles is surrounded by a layer of  $\text{TiO}_2$  in the supported samples. The surface of  $\chi\% \text{TiO}_2/\text{HZSM-5}$  is fairly rough after loading of  $\text{TiO}_2$  as compared to the comparatively smooth surface of HZSM-5 particles. Some small particles can also be found in 60% $\text{TiO}_2/\text{HZSM-5}$ , due to aggregation of excessive  $\text{TiO}_2$ .

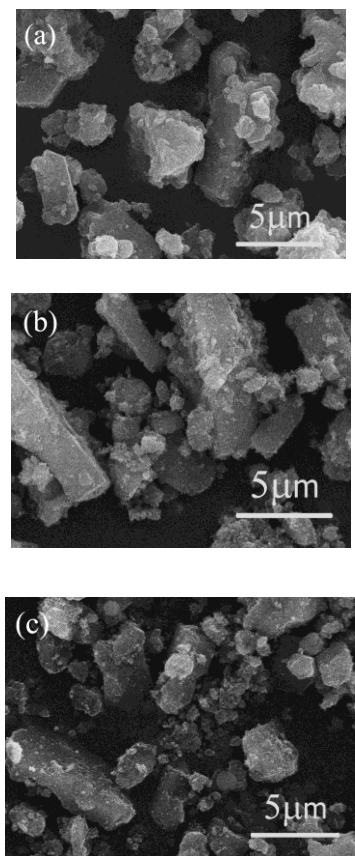


Fig. 2. SEM images of  $\chi\% \text{TiO}_2/\text{HZSM-5}$ : (a) 30% $\text{TiO}_2/\text{HZSM-5}$ , (b) 40% $\text{TiO}_2/\text{HZSM-5}$ , (c) 60% $\text{TiO}_2/\text{HZSM-5}$

BET surface areas of  $\chi\% \text{TiO}_2/\text{HZSM-5}$  and  $\text{TiO}_2$  are presented in Table 1. The pure  $\text{TiO}_2$  has a small surface area of  $36.5 \text{ m}^2/\text{g}$ . HZSM-5 has large surface area due to its porous structure. The supported  $\chi\% \text{TiO}_2/\text{HZSM-5}$  also has larger surface area than pure  $\text{TiO}_2$ , depending on  $\text{TiO}_2$  loading content. As can be seen from the figure, specific surface area of  $\chi\% \text{TiO}_2/\text{HZSM-5}$  increases with decreasing  $\text{TiO}_2$  loading content. Obviously, most of the surface area is provided by the zeolite. On the other hand, it can be concluded that the inner pores inside HZSM-5 are not blocked after loading  $\text{TiO}_2$  on the external surface of the zeolite.

Table 1. BET surface areas of  $\chi\% \text{TiO}_2/\text{HZSM-5}$  and  $\text{TiO}_2$

Samples	$S_{\text{BET}}/\text{m}^2 \cdot \text{g}^{-1}$
$\text{TiO}_2$	36.5
20% $\text{TiO}_2/\text{HZSM-5}$	264.8
30% $\text{TiO}_2/\text{HZSM-5}$	207.6
40% $\text{TiO}_2/\text{HZSM-5}$	205.5
60% $\text{TiO}_2/\text{HZSM-5}$	175.6
70% $\text{TiO}_2/\text{HZSM-5}$	142.3

Fig. 3(a) shows N<sub>2</sub> desorption isotherms of TiO<sub>2</sub> and 40%TiO<sub>2</sub>/HZSM-5. N<sub>2</sub> desorption amount smoothly goes up with the increase of N<sub>2</sub> partial pressure until a sharp increment occurs at N<sub>2</sub> partial pressure of 0.8. That means both of the two materials contain mesoporous structure although the 40%TiO<sub>2</sub>/HZSM-5 has larger adsorption capacity than that of TiO<sub>2</sub>. Capillary condensation of N<sub>2</sub> molecules in mesopores or macropores of the materials leads to the sharp increase of N<sub>2</sub> desorption amount at relatively higher partial pressure.

Fig. 3(b) shows BJH pore size distribution in TiO<sub>2</sub> and 40%TiO<sub>2</sub>/HZSM-5. Most of the pores are in the range of mesoporous size, although the zeolite should have a certain amount of micropores in the cage of HZSM-5. The average pore sizes of TiO<sub>2</sub> and 40%TiO<sub>2</sub>/HZSM-5 are 9.77 nm and 6.70 nm, as calculated according to BJH method. Total pore volumes of TiO<sub>2</sub> and 40%TiO<sub>2</sub>/HZSM-5 are 0.1896 mL/g and 0.2172 mL/g, respectively. Smaller pore size and larger total pore volume are obtained after the addition of HZSM-5.

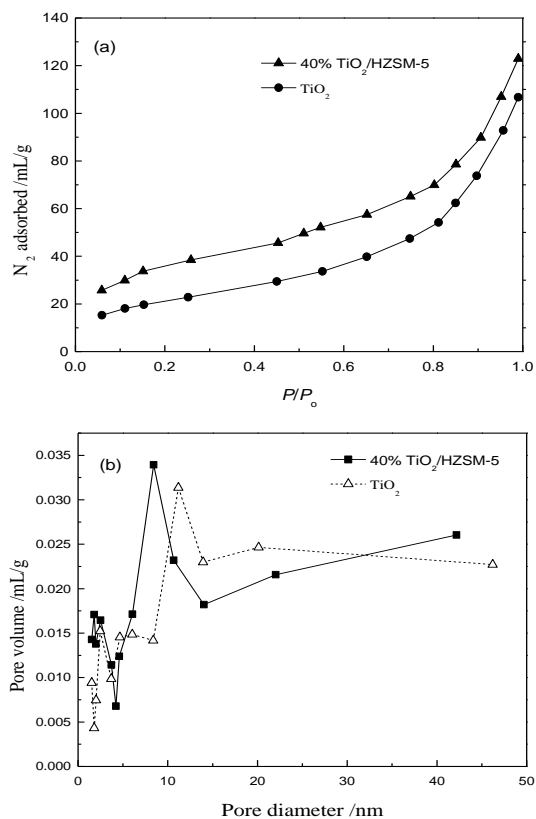


Fig. 3. N<sub>2</sub> desorption isotherms (a) and BJH pore size distribution (b) of TiO<sub>2</sub> and 40%TiO<sub>2</sub>/HZSM-5

Fig. 4 shows adsorption and photocatalytic degradation of methyl orange on  $\chi\%$ TiO<sub>2</sub>/HZSM-5 as a factor of TiO<sub>2</sub> loading content. Photocatalytic reaction time was 30 min under irradiation. As can be seen from the figure, adsorption and degradation of methyl orange lead to total decoloration of the dye molecules. TiO<sub>2</sub> loading

content has influence on both of adsorption capacity and photocatalytic activity of the supported materials. Adsorption of methyl orange on the materials is around 5% while the highest value occurs in the sample contains 40% of TiO<sub>2</sub>. Photocatalytic degradation of methyl orange also varies with increasing TiO<sub>2</sub> loading content. 40%TiO<sub>2</sub>/HZSM-5 has the maximum activity that is as high as 53% after 30 min of irradiation.

Photocatalytic degradation of methyl orange is the major way leading to decoloration of the dye. The supported materials normally have better photocatalytic activity than pure TiO<sub>2</sub>. As indicated before, nano sized TiO<sub>2</sub> is synthesized on the surface of HZSM-5. The well dispersion of TiO<sub>2</sub> can provide more surface area for possible absorption of irradiating photons and the adsorption of methyl orange molecules. The constant incoming irradiation can therefore be absorbed more efficiently as the initial step of photocatalytic degradation. The recombination of photogenerated electrons and holes may be retarded since the zeolite is believed to transfer the electrons much quickly to extend lifetime of the holes [18].

The optimal TiO<sub>2</sub> loading content, i.e. 40%, is due to complex reasons. The improved absorption of irradiating photons after supporting TiO<sub>2</sub> on HZSM-5 are responsible to the enhanced photocatalytic activity on methyl orange degradation. However, since the photocatalyst powders are suspended in the solution, the HZSM-5 may also act to screening the incoming photons. Therefore, after reaching the optimum value, photocatalytic degradation activity of the  $\chi\%$ TiO<sub>2</sub>/HZSM-5 sharply decreases with further addition of HZSM-5.

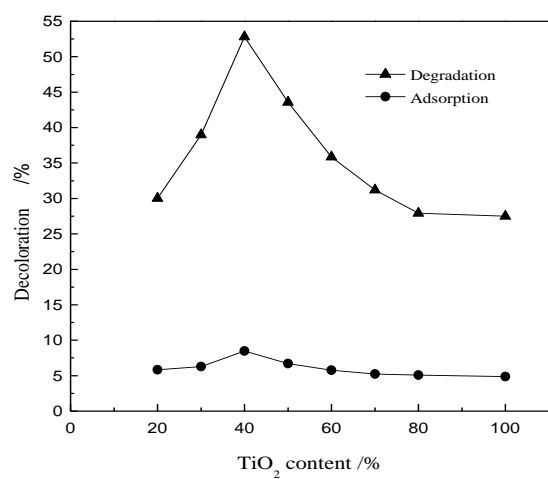


Fig. 4. Adsorption and degradation of methyl orange on  $\chi\%$ TiO<sub>2</sub>/HZSM-5. Photocatalytic reaction time was 30 min under irradiation

#### 4. Conclusion

HZSM-5 was used to support TiO<sub>2</sub> photocatalyst by solvothermal method. The synthesized TiO<sub>2</sub> is in the

anatase phase with nano scale crystallite size. The greatly enlarged surface area is provided by the zeolite after the addition of HZSM-5. Most of the surface of HZSM-5 particles is surrounded by a layer of TiO<sub>2</sub> in the supported samples. The average pore sizes of TiO<sub>2</sub> and 40%TiO<sub>2</sub>/HZSM-5 are 9.77 nm and 6.70 nm. The supported materials normally have better photocatalytic activity than pure TiO<sub>2</sub>.

### Acknowledgement

This work was supported by the Natural Science Foundation of Liaoning Province (No. 2015020186), and the open research fund of Key Laboratory of Wastewater Treatment Technology of Liaoning Province, Shenyang Ligong University (No. 4771004kfs38).

### References

- [1] R. Portela, M. C. Canela, B. Sanchez, F. C. Marques, A. M. Stumbo, R. F. Tessinari, J. M. Coronado, S. Suarez, *Appl. Catal. B* **84**, 643 (2008).
- [2] A. V. Rosario, E. C. Pereira, *Appl. Catal. B* **144**, 840 (2014).
- [3] S. M. López, M. C. Hidalgo, J. A. Navío, *Appl. Catal. A* **404**, 59 (2011).
- [4] W. J. Zhang, J. W. Bai, *Appl. Surf. Sci.* **258**, 2607 (2012).
- [5] Y. J. Wang, J. Lin, R. L. Zong, J. He, Y. F. Zhu, *J. Mole. Catal. A* **349**, 13 (2011).
- [6] D. D. Pang, L. Qiu, Y. T. Wang, R. S. Zhu, F. Ouyang, *J. Environ. Sci.* **33**, 169 (2015).
- [7] X. Liu, K. K. Iu, J. K. Thomas, *Chem. Phys. Lett.* **195**, 163 (1992).
- [8] V. D. Kumari, M. Subrahmanyam, K. V. Subba Rao, A. Ratnamala, M. Noorjahan, K. Tanaka, *Appl. Catal. A* **234**, 155 (2002).
- [9] W. J. Zhang, F. F. Bi, Y. Yu, H. B. He, *J. Mol. Catal. A* **372**, 6 (2013).
- [10] W. J. Zhang, K. L. Wang, Y. Yu, H. B. He, *Chem. Eng. J.* **163**, 62 (2010).
- [11] H. Chen, A. Matsumoto, N. Nishimiya, K. Tsutsumi, *Colloids Surf.* **157**, 295 (1999).
- [12] M. V. Phanikrishna Sharma, K. Lalitha, V. Durga Kumari, M. Subrahmanyam, *Sol. Energy Mater. Sol. Cells* **92**, 332 (2008).
- [13] M. V. Phanikrishna Sharma, V. Durga Kumari, M. Subrahmanyam, *J. Hazard. Mater.* **160**, 568 (2008).
- [14] M. V. Phanikrishna Sharma, V. Durga Kumari, M. Subrahmanyam, *Chemosphere* **72**, 644 (2008).
- [15] M. Nikazar, K. Gholivand, K. Mahanpoor, *Desalination* **219**, 293 (2008).
- [16] L. Zhu, Z. Meng, G. Trisha, W. C. Oh, *Chin. J. Catal.* **2**, 254 (2012).
- [17] W. J. Zhang, X. B. Pei, B. Yang, H. B. He, *J. Adv. Oxid. Technol.* **17**, 66 (2014).
- [18] M. A. O'Neill, F. L. Cozens, N. P. Schepp, *J. Phys. Chem. B* **105**, 12746 (2001).

\*Corresponding author: wjzhang@aliyun.com